MOLECULAR AND CELLULAR BIOLOGY, Nov. 1992, p. 5159–5173
0270-7306/92/115159-15$02.00/0

Vol. 12, No. 11

C-Terminal Truncation of RAP1 Results in the Deregulation of Telomere Size, Stability, and Function in *Saccharomyces cerevisiae*

GABRIELE KYRION,[1] KEN A. BOAKYE,[1] AND ARTHUR J. LUSTIG[1,2]*

Program in Molecular Biology, Sloan-Kettering Institute, Memorial Sloan-Kettering Cancer Center,[1] and Graduate Program in Molecular Biology Cornell University Graduate School of Medical Sciences,[2] New York, New York 10021

Received 22 May 1992/Returned for modification 1 July 1992/Accepted 12 August 1992

The *Saccharomyces cerevisiae* DNA-binding protein RAP1 is capable of binding in vitro to sequences from a wide variety of genomic loci, including upstream activating sequence elements, the *HML* and *HMR* silencer regions, and the poly($G_{1-3}T$) tracts of telomeres. Recent biochemical and genetic studies have suggested that RAP1 physically and functionally interacts with the yeast telomere. To further investigate the role of RAP1 at the telomere, we have identified and characterized three intragenic suppressors of a temperature-sensitive allele of *RAP1*, *rap1-5*. These telomere deficiency (*rap1^t*) alleles confer several novel phenotypes. First, telomere tract size elongates to up to 4 kb greater than sizes of wild-type or *rap1-5* telomeres. Second, telomeres are highly unstable and are subject to rapid, but reversible, deletion of part or all of the increase in telomeric tract length. Telomeric deletion does not require the *RAD52* or *RAD1* gene product. Third, chromosome loss and nondisjunction rates are elevated 15- to 30-fold above wild-type levels. Sequencing analysis has shown that each *rap1^t* allele contains a nonsense mutation within a discrete region between amino acids 663 and 684. Mobility shift and Western immunoblot analyses indicate that each allele produces a truncated RAP1 protein, lacking the C-terminal 144 to 165 amino acids but capable of efficient DNA binding. These data suggest that RAP1 is a central regulator of both telomere and chromosome stability and define a C-terminal domain that, while dispensable for viability, is required for these telomeric functions.

Telomeres, the structures present at the ends of linear eukaryotic chromosomes, are essential for the stability and complete replication of the chromosome. Telomeric DNA, at its extreme terminus, is composed of a variable number of simple sequence repeats. These repeats usually contain a G-rich strand, oriented in a 5′-to-3′ direction toward the terminus. In contrast to other genomic sequences, telomeres are replicated inexactly. The size and, in some organisms, the sequence of an individual telomere vary among different cells of a population (60). The average size of telomeric DNA appears to be maintained through a regulated equilibrium between the loss and gain of telomeric sequences (36, 45, 46, 60). One component involved in this process is the ribonucleoprotein complex telomerase (16–18, 37, 48, 49, 59). This enzyme, identified in both ciliate and mammalian cells, is capable of catalyzing the addition of the G-rich simple sequences onto the 3′ end of single-stranded substrates, utilizing a sequence within its RNA component as a template. A similar activity is likely to explain the properties of telomere addition in yeasts and other organisms in which telomerase has not yet been identified (60). The essentiality of maintaining telomeric sequences is underscored by the recombinational instability, chromosome loss, and lethality caused by loss of part or all of telomeric DNA (34, 60).

Telomeres are packaged in vivo into unique nonnucleosomal complexes, formed in part by the association between telomeric DNA and specific nonhistone telomere-binding proteins (2, 5, 14, 15, 41–44, 58). Although the functions of these complexes remain unknown, they are likely to participate in the regulation of telomere size and stability, possibly by controlling the accessibility of the telomere to terminal addition, degradation, or recombination.

Proteins capable of specific binding to telomeric DNA have been identified in a number of organisms, including ciliates, protists, yeasts, and humans (4, 9, 19, 32, 33, 41). The most abundant telomere-binding activity of the yeast *Saccharomyces cerevisiae* is the multifunctional protein RAP1 (4, 33, 50). RAP1 binds in vitro to sequences from a variety of genomic loci, including the upstream activating sequences of a large number of genes, the silencer regions adjacent to the cryptic mating-type information present at *HML* and *HMR*, and sites embedded within the telomeric poly($G_{1-3}T$) tracts. The phenotypes of both *rap1* mutants and strains overproducing RAP1 have demonstrated that this protein is likely to act in all three functions in vivo (8, 12, 20, 28, 35, 54). Although disruptions within the *RAP1* gene result in cellular inviability (50), the essential function of *RAP1* has not been identified. The mechanism of RAP1 action in these seemingly disparate roles remains unknown.

Several lines of evidence suggest a functional role for RAP1 at the telomere. First, recessive *rap1^{ts}* mutations that exhibit temperature-dependent decreases in poly($G_{1-3}T$) tract size have been identified (8, 35). Conversely, overproduction of RAP1 results in a dose-dependent elongation of telomere tracts (8). Second, mutations within RAP1 binding sites of synthetic telomeres result in a significant decrease in the efficiency and fidelity of telomere addition in a plasmid telomere healing assay (35). Finally, RAP1 has been identified in telomeric chromatin fractions (8, 58).

In this report, we describe the genetic and molecular characterization of three novel intragenic suppressors of a temperature-sensitive *rap1* allele (28, 36). These suppressors (called *rap1^t* to indicate telomere deficiency) result both in

* Corresponding author.

promiscuous telomere elongation and deletion and in chromosome destabilization. The molecular characterization of these suppressors has identified a C-terminal domain critical for the regulation of telomere size in yeast cells.

MATERIALS AND METHODS

Plasmids. Plasmid p784.4 (kindly provided by C. Newlon and V. Zakian) contains a 3.5-kb *Eco*RI fragment derived from sequences ≈2.3 to 5.8 kb from the left arm of chromosome III ($cIII_L$) (39). pKB1 and pKB2 contain the telomere-proximal 900-bp *Eco*RI-*Sal*I fragment of p784.4 and the 2.3-kb *Sal*I fragment of p784.4, respectively, subcloned into pUC19. pKB2 also has weak homology to one of the telomeres of chromosome XI.

pUC19/1-17, pUC19/1-18, and pUC19/1-19 contain the polymerase chain reaction (PCR)-amplified *Eco*RI fragments (see below) from *rap1-17*, *rap1-18*, and *rap1-19* strains, respectively, cloned into the *Eco*RI site of pUC19, so that the downstream *Eco*RI site is adjacent to the *Xba*I site within the polylinker. pM1-11 is a centromeric plasmid containing *TRP1* and *ARS1* sequences (28) and has a unique *Eco*RI cloning site. pD130 (kindly provided by D. Shore) contains the wild-type *RAP1* gene cloned into the *Eco*RI site of pM1-11 (28). Plasmids pM1-11/1-17, pM1-11/1-18, and pM1-11/1-19 contain the *Eco*RI fragments from pUC19/1-17, pUC19/1-18, and pUC19/1-19, respectively, cloned into pM1-11.

$pRS316_H$ is identical to the *URA3*-containing centromeric (CEN) plasmid pRS316 (52) except for elimination of the unique *Hin*dIII site by a filling-in reaction. $pRS316_H$/1-5 was derived by cloning the *Eco*RI-*Xba*I fragment, containing the *rap1-5* gene, from pUC19/*rap1-5* (kindly provided by D. Shore) into $pRS316_H$. For restriction fragment substitutions, the 1.2-kb *Sph*I-*Xba*I fragments (containing the C-terminal third of *RAP1*) from pUC19/1-17, pUC19/1-18, and pUC19/1-19 were used to replace the corresponding fragments in $pRS316_H$1-5. The *Sph*I-*Xba*I fragments of the cloned *rap1^t* alleles are 75 bp smaller than the corresponding *rap1-5* fragment, since the *Xba*I site is derived from polylinker sequences 25 bp downstream of the *Eco*RI site in pUC19. The resulting plasmids ($pRS316_H$/1-17, $pRS316_H$/1-18, and $pRS316_H$/1-19) contain wild-type *RAP1* information from the natural *Eco*RI site (nucleotide −407) to the internal *Sph*I site (nucleotide 2360) and *rap1^t* information from the *Sph*I site (nucleotide 2360) to nucleotide 3575 in the 3′ noncoding region (see Fig. 8).

pRS315/RAP was formed by ligation of the *Eco*RI-*Xba*I fragment of *RAP1* into the polylinker of the *LEU2*-containing CEN plasmid pRS315 (52). pV-R-URA3-TEL and padh: URA3-TG (kindly provided by D. Gottschling) were used to position *URA3* adjacent to both telomeric and nontelomeric poly(G_{1-3}T) tracts (13).

Yeast strains and growth. All of the studies described here were conducted with strains isogenic to W303α (*MAT*α *ura3-1 his3-11,15 leu2-3,112 trp1 ade2-1 can1-100*). The *rap1-5* strains YDS410 and YDS411, as well as isogenic backcrossed derivatives of these strains, were used for the generation of suppressors (28, 35). Haploid strains used for determination of the rates of artificial chromosome (AC) loss were derived from sporulation of diploids having the genotype *MAT*α/*MAT***a** *ade2-1*/*ade2-1 trp1*/*trp1 ura3-1*/*ura3-1 HIS3*/*his3 leu2-3,112*/*leu2-3,112* AC: *SUP11 URA3* but different *RAP1* genotypes. AJL273 is heterozygous for *rap1-18*; AJL274, AJL278, and AJL307 are heterozygous for *rap1-17*; AJL283 and AJL284 are heterozygous for *rap1-5*; and AJL 275 and AJL306 are homozygous for the wild-type copy of *RAP1*.

Diploid strains used for chromosome loss assays were AJL306, AJL307, AJL308 (*rap1-17*/*rap1-17*; otherwise isogenic to AJL306), and AJL308/RAP (derived from AJL308 by the introduction of pRS315/RAP). Strains used for PCR amplification and extract isolation were AJL274-1d (*rap1-17*), AJL256-16d (*rap1-18*), and SG38 (*rap1-19*). Strain YDS203-2d [*MAT*α *RAP1*::*LEU2* pD145 (CEN *RAP1 URA3 SUP4-o*) *ade2-1 his3-11,15 leu2-3,112 trp1-1 ura3-1*] has been previously described (28). Strains GK15, GK16, GK17, GK18, GK19, GK20, GK21, and GK22 are isogenic to YDS203-2d but contain plasmids pM1-11/1-17, pM1-11/1-18, pM1-11/1-19, pD130, $pRS316_H$/1-17, $pRS316_H$/1-18, $pRS316_H$/1-19, and $pRS316_H$/1-5, respectively, in place of pD145 and were derived by plasmid shuffles (3, 28; see below).

The *URA3* gene was introduced into a wild-type strain adjacent to a truncated version of chromosome V as previously described (13). To generate *rap1-17* strains containing this marked telomere, transformants were crossed to AJL278-4d (*MAT***a** *rap1-17 ade2-1 ura3-1 HIS3 leu2-3,112 trp1*), and the subsequent diploid was sporulated. The *URA3* gene, in the presence of an adjacent 80-bp poly(G_{1-3}T) tract, was introduced into the *ADH4* gene as previously described (13). Transformants were crossed to AJL278-4d, and the resulting diploids were sporulated. In each case, the structures of the relevant regions were confirmed by both Southern and genetic analyses.

For the introduction of *rad1* and *rad52* mutations, W839-11D (*MAT*α *RAP1 ade2-1 ura3-1 his3 rad52*::*TRP1 rad1*::*LEU2*; kindly provided by R. Rothstein) was crossed to AJL278-4d, and the resulting diploid (AJL330) was sporulated. *rap1-17 rad52*, *rap1-17 rad1*, and *rap1-17 rad1 rad52* strains were identified by detection of nonparental ditype tetrads.

Methods for the manipulation of yeast strains and for the preparation of media were as described elsewhere (47). For subculturing studies, strains were grown on solid media, each round of subculturing proceeding through growth of a single colony (35, 36).

Generation of cold-sensitive suppressors of temperature-sensitive lethality. For the identification of spontaneous suppressors of temperature-sensitive lethality, ≈10^5 cells, derived from independent colonies of *rap1-5*-containing cells, were spread onto individual YPD plates, and the plates were incubated at 37°C for 3 to 5 days. Colonies capable of growth at 37°C were identified and replated at 37°C. Candidate suppressors were subsequently tested for the ability to grow at a variety of temperatures. After screening of ≈750 temperature-resistant derivatives of *rap1-5*, eight strains that conferred slow growth at 25°C were identified. Of these, three suppressors (*rap1-17*, *rap1-18*, and *rap1-19*; collectively termed the *rap1^t* alleles) that had substantially increased telomere tract length and heterogeneity were identified. All three suppressors segregated 2:2 for both growth rate and telomere tract elongation in crosses to *rap1-5* and wild-type strains and for temperature-sensitive suppression in crosses to *rap1-5* strains. Cosegregation of the phenotypes was maintained over repetitive rounds of backcrossing.

Identification of telomere fragment lengths. Overall telomere fragment lengths were determined by probing blots of *Xho*I-digested genomic DNA with nick-translated poly(dG-dT) · poly(dC-dA) [poly(GT)] (36). In these blots, telomeres adjacent to the subtelomeric Y′ element, containing a conserved *Xho*I site, give rise to fragments that contain 870 bp

of Y′ sequence and a variable length of poly($G_{1-3}T$) tract (XY′-class telomeres; 46). Telomeres that contain only the X subtelomeric repeat (X-class telomeres) lack the conserved *Xho*I site and therefore give rise to larger telomeric fragments.

For identification of telomere fragment lengths on $cIII_L$, DNA was digested with *Sal*I, which cleaves 3.2 kb from the left terminus of chromosome III (39). Subsequently, Southern blots were probed with either pKB1 or the 900-bp *Eco*RI-*Sal*I fragment (telomere proximal to the *Sal*I site) derived from p784.4. Mean telomere lengths were determined by measuring the midpoint of the telomeric fragment distribution. Telomere heterogeneity was determined by measuring the difference between the largest and smallest fragments within this distribution.

In genomic blots of *Sal*I digests, the 2.3-kb *Sal*I fragment of pKB2 hybridizes predominantly to an internal fragment of identical size that is located just telomere distal to the terminal *Sal*I site on $cIII_L$. However, this fragment also has weak homology to a telomeric fragment that we have mapped by transverse alternating-field electrophoresis (TAFE) to chromosome XI (data not shown). The chromosome XI (cXI) fragment was determined to be telomeric by both its size heterogeneity, typical of telomeric fragments, and its sensitivity to nuclease BAL 31 digestion. This homology, which is the likely consequence of a degenerate X repeat located in the 2.3-kb *Sal*I fragment (39), allowed us to determine the fragment lengths of the cXI telomere.

Determination of rapid deletion events. Strains containing either the *rap1-17* or *rap1-18* allele were subcultured, and the fragment lengths of $cIII_L$ telomeres were determined. The lengths of most $cIII_L$ telomeric fragments in these populations ranged from 3 to 4 kb. These cells were plated, and individual colonies were identified after ≈25 generations of growth. DNA was then isolated from 150 individual colonies (50 from each of two *rap1-17* strains and 50 from a *rap1-18* strain), and the telomere fragment length of the $cIII_L$ telomere was determined. Blots were stripped and reprobed with pKB2. The predominant species on these blots is the 2.3-kb *Sal*I fragment, demonstrating the absence of partial *Sal*I digestion products. These blots also served to determine telomeric fragment sizes from one of the cXI telomeres.

Nuclease BAL 31 digestions and tract length determination. Nuclease BAL 31 digestions were performed as described previously (57). High-molecular-weight DNA was digested first with nuclease BAL 31, under the conditions indicated in the legend to Fig. 4, and then with *Sal*I. The resulting blots were probed with pKB1, which identifies the left telomere of chromosome III. Blots were subsequently stripped and probed with sequences capable of hybridization to internal restriction fragments. In every case, the mobilities of internal fragments were unchanged under conditions in which telomeric fragments were degraded by nuclease BAL 31. To determine tract length, blots were stripped and reprobed with poly(GT). The tract length was determined by measuring the extent of nuclease BAL 31 digestion required to eliminate hybridization to poly(GT).

Chromosome loss assays. An artificial chromosome containing the entire $cIII_L$ and a telocentric right arm containing the *SUP11* and *URA3* genes was introduced into W303α as previously described (53). Candidate transformants were screened by restriction and TAFE analysis for the expected 150-kb chromosome fragment (11). This strain was subsequently crossed to either a wild-type, *rap1-5*, *rap1-17*, or *rap1-18* strain. Wild-type and mutant strains containing the artificial chromosome were identified after sporulation of the resulting diploids.

As expected, wild-type and *rap1-5* cells produce white colonies on low-adenine synthetic medium (22, 24). In contrast, *rap1-17*, *rap1-18*, and *rap1-19* strains all display a weaker level of ochre suppression, giving rise to pink colonies on low-adenine medium. Although the cause of this reduction in suppression is not yet understood, it is not dependent on the position of *SUP11* near the telomere of the artificial chromosome, since circular plasmids containing the *SUP11* gene show an identical reduction in ochre suppression (data not shown). This property permits the visualization of 2:0 (white:red) and 1:0 (pink:red) segregation events in haploid strains. To confirm these identifications, white and pink colonies were crossed to a wild-type strain lacking the artificial chromosome, and the segregation of Ura and Ade markers in tetrads derived from the resulting diploid was analyzed. Diploids derived from pink colonies segregated 2:2 (Ura^+ Ade^+:Ura^- Ade^-), while those derived from white colonies predominantly segregated 4:0 (Ura^+ Ade^+:Ura^- Ade^-). Restriction and TAFE analyses were also used to confirm the presence or absence of the artificial chromosome. Diploid strains carrying the artificial chromosome have similar characteristics. Wild-type or heterozygous diploid strains containing zero, one, or two copies of the chromosome yield red, pink, or white colonies, respectively. In contrast, homozygous *rap1*^{t}/*rap1*^{t} cells produce orange colonies, while loss and gain events give rise to red and pink colonies, respectively. These copy numbers were confirmed in a subset of diploids through the analysis of Ura and Ade markers in tetrads following sporulation. In addition, all red colonies tested were Ura^- and lacked the artificial chromosome, as determined by TAFE analysis.

Two methods were used to determine the rate of chromosome loss. First, the overall rate of loss was determined by the method of the median (22, 30). For each experiment, 10 colonies of identical size (0.3 to 0.4 mm), following growth at 25°C on either low-adenine or YPD medium, were suspended in low-adenine medium, and part or all of the colony was subsequently spread onto low-adenine plates. A proportion of each colony was diluted and plated on complete medium to obtain an estimate of the total cells within each colony. No significant differences between the growth of colonies containing or lacking the artificial chromosome were observed under either set of growth conditions. Identical loss rates were observed regardless of whether colonies were grown on low-adenine or rich medium before fluctuation analysis. Fluctuation analysis was performed in multiple wild-type, *rap1-5*, and *rap1-17* haploid strains and in multiple trials of wild-type and homozygous *rap1-17*/*rap1-17* diploids.

As a second independent technique, the overall loss rate and the frequencies of 2:0 and 1:0 segregation events were determined by half-sector analysis in wild-type and *rap1-17* strains (24). Rates determined by sectoring and fluctuation analysis did not differ by more than twofold.

Subcloning and functional expression of *rap1*^{t} alleles. The mutant *rap1*^{t} genes (*rap1-17*, *rap1-18*, and *rap1-19*) were amplified from strains carrying these alleles by PCR, using primers flanking the gene (1). Both upstream and downstream primers contained mismatches which created unique *Eco*RI sites flanking the amplified gene (see Fig. 8). The upstream and downstream primers were located at positions 508 to 534 and 3561 to 3579, respectively. The PCR products were fractionated on agarose gels, and the full-length product was electroeluted and precipitated.

For functional studies, pM1-11/1-17, pM1-11/1-18, and

pM1-11/1-19 were transformed into yeast strain YDS203-2d by spheroplast transformation (47). A plasmid shuffle was then conducted by selection of canavanine-resistant cells (28). The absence of the wild-type plasmid was confirmed by Southern analysis. These strains contain the PCR-amplified genes as the sole source of RAP1. Similarly, $pRS316_H$/1-17, $pRS316_H$/1-18, $pRS316_H$/1-19, and $pRS316_H$/1-5 were transformed into strain GK18 by the lithium acetate method (47). A plasmid shuffle was then performed by screening unselected cells for the Trp^- phenotype, giving rise to strains GK19 to GK22, respectively. These strains contain the *rap1-5* gene (GK22) or the hybrid genes (GK19 to GK21) as the sole source of RAP1.

DNA sequencing. Double-strand sequencing of the *Sph*I-*Xba*I fragment from pUC19/1-17, pUC19/1-18, and pUC19/1-19 was performed by standard techniques (1), using overlapping sets of primers spaced at ≈300-bp intervals. The region between the *Sph*I site and sequences downstream of the nonsense codons was sequenced on both strands in each case. Further sequencing of the *rap1-17* gene demonstrated the absence of any other mutations in the *Sph*I-*Xba*I fragment. The primers used for the sequence of the coding strand were as follows: primer 1A, positions 2311 to 2329; primer 2A, positions 2585 to 2600; primer 3A, positions 2832 to 2848; primer 4A, positions 3101 to 3118; and primer 5A, positions 3298 to 3310. The primers used for the sequence of the noncoding strand were as follows: primer 1B, 2603 to 2623; primer 2B, 2872 to 2889; primer 3B, 3131 to 3147; primer 4B, 3387 to 3403; and primer 5B, universal upstream primer for M13 (New England Biolabs).

Mobility shift assays. Yeast whole-cell extracts were isolated by liquid nitrogen lysis (1). Extracts were isolated from the original wild-type and *rap1^t* strains as well as from strains carrying the cloned *rap1^t* allele on CEN plasmids as the sole source of RAP1 (GK19, GK20, and GK21). Binding reactions were performed for 20 min at 25°C as described previously (35, 51), using 1 to 5 μl of extract, 0.5 μg each of poly(dI-dC) and pUC19 as nonspecific competitors, and 0.13 ng of ^{32}P-labeled AT13 (see below) in each reaction. Products were subjected to electrophoresis for 2 h at 10 V/cm on 4% (40:1) polyacrylamide gels containing 5% glycerol and 0.5× Tris-borate-EDTA.

Substrates for binding (AT12, AT13, and TEF2) were prepared by annealing single-stranded oligonucleotides (4, 35), producing double-stranded substrates that contain a GAT or GATC 5′ overhang. To generate labeled AT13 substrate, this overhang was filled in with Klenow enzyme, using [^{32}P]dCTP as the labeled nucleotide. The sequence of the C-rich strand of AT13 (35) is CCCACACACACA<u>CACCCACACACA</u>CACACACACCACACATGACGCGT, the underline referring to the position of the RAP1 binding site, which is a 12-of-13-base match to the RAP1 consensus sequence. The sequence of the C-rich strand of the nontelomeric RAP1 binding site, TEF2 (4), is GATCCCATTCAT GT<u>GCACCCACACATTT</u>AG, the underline referring to the RAP1 consensus sequence. The sequence of the C-rich strand of AT12 is CCCACACACACACACACACACA(C)A CACACACACACCACACATGACGCGT. AT12 contains a mutation within the AT13 sequence that eliminates RAP1 binding. Previous studies have shown that a subpopulation of AT12 molecules contains a T residue in the position of the C residue indicated by the parentheses (35). Competitions were performed as described above, using a one- to eightfold molar excess of unlabeled AT12, AT13, or TEF2.

Western immunoblot analysis. Denatured yeast extracts were prepared as described previously (26). Extracts and prestained protein standards (Bio-Rad) were fractionated on a 9% sodium dodecyl sulfate (SDS)-polyacrylamide gel, and the gel was electroblotted onto an Immobilon P filter (Millipore). Western analysis was carried out as described previously (1). Primary immunobinding was performed for 16 h at 4°C, using a 1/3,000 dilution of mouse polyclonal antibodies directed against wild-type RAP1 (kindly provided by D. Shore). Bound antibody was detected by incubation with an alkaline phosphate–anti-mouse immunoglobulin conjugate (Organon Teknika) and visualized by reaction with nitroblue tetrazolium and 5-bromo-4-chloro-3-indolylphosphate toluidium.

RESULTS

Identification of cold-sensitive suppressors of *rap1-5*. To investigate the role of RAP1 at the telomere, we sought to identify suppressors of both the temperature sensitivity and the telomere phenotypes of the *rap1-5* allele. Strains containing the *rap1-5* allele grow at wild-type rates at the permissive temperature, 25°C, but cease growth after several generations at the restrictive temperature, 37°C (28). Previous studies have demonstrated that cells containing this allele display a 150-bp increase in telomere tract size at 25°C while exhibiting a decrease in tract length following growth at semipermissive temperatures (35).

Three intragenic suppressors of *rap1-5* (*rap1-17*, *rap1-18*, and *rap1-19*) that suppressed temperature sensitivity and conferred unique telomere length phenotypes were identified. As a consequence of their similar phenotypes, we will refer to these suppressors collectively as the *rap1^t* alleles. Each of the *rap1^t* alleles confers a growth rate ≈2-fold slower (1.7-, 1.8-, and 2.1-fold for *rap1-17*, *rap1-18*, and *rap1-19* strains, respectively) than that exhibited by either wild-type or *rap1-5* strains at 25°C and is capable of growth at the previously restrictive temperature, 37°C. The slow growth rate at 25°C is recessive to both *rap1-5* and wild-type alleles, while suppression of temperature sensitivity at 37°C is dominant to the *rap1-5* allele (data not shown).

Three lines of evidence indicate that these mutations represent intragenic suppressors of the *rap1-5* mutation. First, the mutations are tightly linked to the *RAP1* gene. In crosses of each *rap1^t* mutant to a wild-type strain, sporulation of the resultant diploids never yields a *rap1-5^{ts}* spore colony (0 of 160 tetrads for *rap1-17*). Second, complementation of the recessive phenotypes of the *rap1^t* mutants (slow growth and linear chromosome loss [see below]) is conferred by a single copy of wild-type *RAP1* gene on a CEN plasmid (Table 1; data not shown). Third, characterization of the cloned *rap1^t* alleles has revealed that each mutation lies within the carboxy-terminal region of the *RAP1* gene (see below).

Characterization of the XY′ class of telomeres in *rap1^t* strains. The behavior of yeast telomeres in the *rap1^t* strains was initially investigated by examining the telomeric fragment lengths of the XY′ class of telomeres. XY′-class telomeres can be visualized as a heterogeneous group of *Xho*I restriction fragments capable of hybridization to poly(GT). In wild-type strains, these fragments are centered at 1.2 kb, representing a telomere tract length of ≈300 bp. In contrast, the *rap1^t* alleles exhibit several unusual telomere length characteristics. First, when cells are grown at 25°C, average telomere length increases to 1 to 3 kb greater than the lengths observed in *rap1-5* cells (Fig. 1A and C; see also Fig. 7A). Subculturing of *rap1^t* cells results in either a maintenance of this distribution or a continuing elongation of

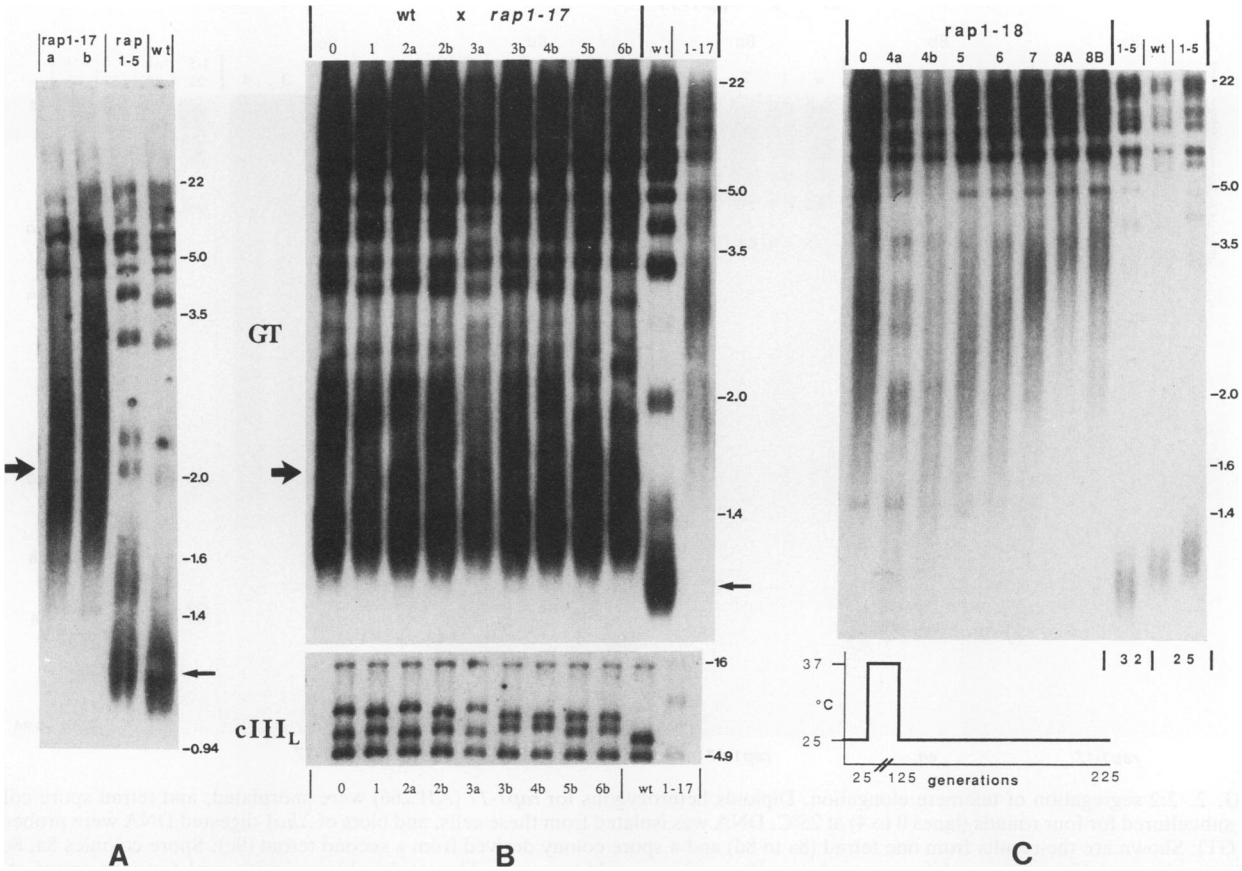

FIG. 1. Semidominant reversible elongation of XY′ telomere conferred by the *rap1^t* alleles. (A) Increases of XY′-class telomere length and heterogeneity in *rap1-17* mutants. Two colonies (a and b) derived from the original strain carrying the *rap1-17* allele, as well as wild-type (wt) and *rap1-5*-containing strains, were grown at 25°C, and the DNA was isolated. DNA was digested with *Xho*I, and genomic blots were hybridized to poly(GT). Arrows on the left and right show the mean sizes (in kilobases in all panels) of XY′-class telomeres in *rap1-17* (a) and wild-type strains, respectively. Size markers are shown on the right. (B) Semidominance of telomere elongation in the *rap1^t* alleles. A strain heterozygous for the *rap1-17* mutation (AJL266), derived from mating of the *rap1-17*(a) strain displayed in panel A to an isogenic wild-type strain, was subcultured for zero to six rounds at 25°C, each round representing the progeny of a single cell derived from the previous round of subculturing. After the first subculturing, two individual colonies (a and b) were subcultured independently for two (2a and 3a) to five (2b to 6b) additional rounds, respectively. Each round represents ≈25 generations of growth. Genomic blots of *Xho*I-digested DNA derived from these cells, as well as from wild-type (wt) and *rap1-17* (1-17) cells, were probed with poly(GT) (GT; top). Arrows on the left and right indicate the mean sizes of XY′-class telomeres in the heterozygous diploids and wild-type haploid strains, respectively. DNAs were digested as described above, and the resulting Southern blot was probed with a chromosome III-specific probe, p784.4 (cIII$_L$; bottom). The largest and smallest species represent internal fragments (with estimated sizes shown on the right), while the intermediate species represent the cIII$_L$ telomeric fragments. We note that the lower degree of heterogeneity of *Xho*I cIII$_L$ telomeric fragments is the consequence of the larger size of these fragments. Similar results were obtained in strains heterozygous for *rap1-18*. (C) Temperature sensitivity and partial reversibility of *rap1^t* telomere tract length. *rap1-18*-containing cells grown at 25°C were subcultured for four rounds at 37°C and subsequently subcultured for an additional four rounds at 25°C (see diagram). DNA was isolated from cells before subculturing (lane 0), after four rounds of subculturing at 37°C (lane 4a), and after each round of subsequent subculturing at 25°C (lanes 4b to 8B). Blots of *Xho*I-digested DNA were subsequently probed with poly(GT). 4a and 4b are separated by less than a complete round of subculturing (<20 generations). 8A and 8B represent two individual colonies derived from the last round of subculturing. DNAs isolated from wild-type (wt) cells grown at 25°C and from *rap1-5* (1-5) cells grown at either 25 or 32°C are shown in the rightmost lanes.

telomere length (Fig. 1C and 2). Telomere elongation is at least partially reversible (Fig. 1C). When cells are shifted to 37°C, telomere size decreases, with some telomeric fragments reattaining lengths close to that of the wild type. As expected, cells shifted back to growth at 25°C regain elongated telomere fragment lengths.

Second, the distribution of telomere fragment lengths in these mutants is dramatically increased. While the XY′ class of telomeres is normally maintained in a distribution of about 300 bp, *rap1^t* telomeres range in size from 150 bp to >4 kb larger than *rap1-5* telomeres. This heterogeneity is achieved after only 20 generations of growth, suggesting that a process capable of rapidly altering telomere size is present in these mutants.

Unlike the growth characteristics conferred by these alleles, telomere elongation is semidominant. The telomeres of diploids heterozygous for the *rap1-17* or *rap1-18* allele are maintained throughout subculturing at sizes intermediate between those of the parental strains (Fig. 1B). After sporulation of these diploids, *rap1^t* spore colonies invariably display elongated and heterogeneous telomeres (Fig. 2). In contrast, wild-type spore colonies, inheriting elongated telomeres from the heterozygous diploid, show an immediate reduction in both telomere heterogeneity and size, with

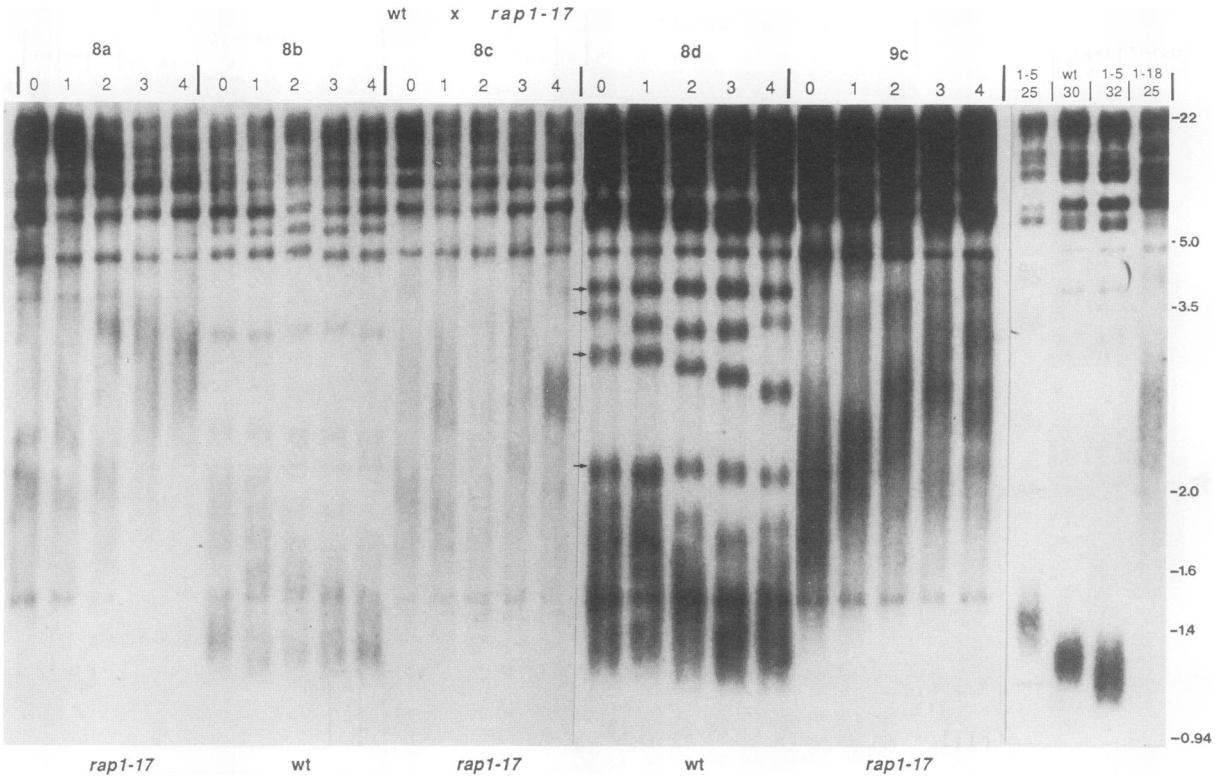

FIG. 2. 2:2 segregation of telomere elongation. Diploids heterozygous for *rap1-17* (AJL266) were sporulated, and tetrad spore colonies were subcultured for four rounds (lanes 0 to 4) at 25°C. DNA was isolated from these cells, and blots of *Xho*I-digested DNA were probed with poly(GT). Shown are the results from one tetrad (8a to 8d) and a spore colony derived from a second tetrad (9c). Spore colonies 8a, 8c, and 9c contain the *rap1-17* mutation, while spore colonies 8b and 8d are wild type (wt). The results obtained with *rap1-5* strains grown at 25 or 32°C, wild-type strains grown at 30°C, and a *rap1-18* strain grown at 25°C are shown in the rightmost lanes. Size markers (in kilobases) are shown on the right. Restriction fragments representing X-class telomeres, lacking the Y′ repeat (indicated by the arrows in spore colony 8d), are visible in wild-type segregants; these fragments either decrease in size, as a consequence of inheriting an elongated telomere, or reattain wild-type lengths within the first round of subculturing, probably as a result of inheritance of telomeres close to wild-type size.

many telomeric fragments reattaining lengths close to or at wild-type lengths.

The *rap1*^{t} mutations result in expansion of telomeric poly($G_{1-3}T$) tracts. To better understand the processes acting at telomeres in these mutants, we analyzed the characteristics of several individual telomeres in two *rap1*^{t} alleles, *rap1-17* and *rap1-18*. (Except where noted, all of the studies described were performed with both strains.)

The telomere fragment lengths present at $cIII_L$ were determined in wild-type, *rap1-5*, and *rap1*^{t} strains (Fig. 1B and 3). *Sal*I digestion of wild-type DNA produces an ≈3.2-kb $cIII_L$ telomeric fragment, terminating in ≈300 bp of poly($G_{1-3}T$) sequence. Diploids formed between wild-type and *rap1*^{t} strains maintain two discrete termini throughout subculturing, one close to wild-type tract length and the other 0.6 to 4 kb larger (Fig. 1B). The behavior of *rap1*^{t} telomeres was analyzed after subculturing of mutant and wild-type spore colonies derived from the heterozygous diploid. In *rap1*^{t} spore colonies that inherit short $cIII_L$ telomeres from the heterozygous diploid, telomeres slowly elongate to mean lengths averaging 2.5 kb (but ranging up to 4 kb) larger than those found in wild-type or *rap1-5* cells (e.g., Fig. 3, spore colony 8c). Similarly, *rap1*^{t} cells that inherit elongated telomeres normally maintain the increased tract size through subsequent subculturing (data not shown). The elongated fragments are selectively degraded by nuclease BAL 31, confirming their telomeric position (Fig. 4A). In contrast, the telomeres of wild-type spore colonies fail to elongate, many telomeres reattaining sizes close to or at wild-type lengths (data not shown; see Discussion).

In addition to the characteristics of the XY′ class of telomeres, several lines of evidence argue that the increase in telomere fragment size is the consequence of increased poly($G_{1-3}T$) tract size rather than an alteration in subtelomeric sequences. First, *rap1*^{t} cells inheriting short $cIII_L$ telomeres from the diploid slowly elongate, an effect most consistent with telomere growth. Second, elongation of telomeres can be partially reversed, as noted below, by a rapid loss of telomeric sequences. Following deletion, these telomeres again slowly reelongate. Third, the different fragment lengths inherited by wild-type spore colonies from heterozygous diploids (e.g., 3.2 kb in spore colony 18b and 3.8 kb in spore colony 16b; Fig. 4) appear to be due to differences in the lengths of poly($G_{1-3}T$) tracts (Fig. 4B). While a telomere having wild-type tract length is incapable of hybridization to poly(GT) after elimination of just 300 bp of terminal sequences by nuclease BAL 31, the elongated fragment still hybridizes to this probe after loss of over 800 bp of terminal sequence. That is, while the initial fragment sizes are significantly different, the length at which hybridization to the telomeric probe is lost is identical. Third, despite the absence of subtelomeric repeats, poly($G_{1-3}T$) tracts, when adjacent to a telomerically positioned *URA3* gene in *rap1-17* cells, increase to lengths 0.5 to 3.0 kb larger

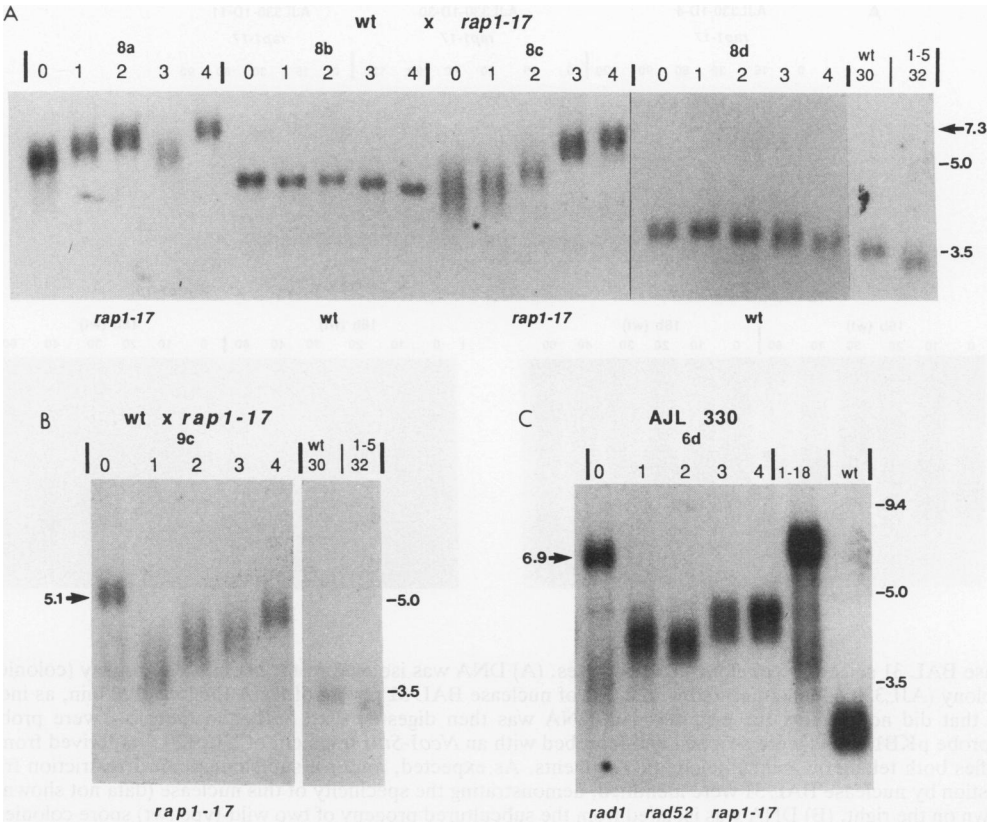

FIG. 3. Behavior of $cIII_L$ telomeres in *rap1-17* and wild-type spore colonies. (A and B) The DNA preparations described in the legend to Fig. 2 were digested with *Sal*I, and the subsequent blots were probed with the 900-bp fragment of p784.4, which visualizes the $cIII_L$ telomere. (C) A strain heterozygous for *rap1-17*, *rad52*, and *rad1* (AJL330) was sporulated, and triple mutant spore colonies (e.g., 6d) were subcultured for four rounds at 25°C (lanes 0 to 4). DNA was isolated and digested with *Sal*I, and the blots were probed with pKB1, which is specific to the $cIII_L$ telomere. Control *rap1-18* and wild-type cells, digested and probed in the same way, are shown on the right. Arrows on the right and left give the estimated sizes (in kilobases) of the $cIII_L$ telomeres of AJL266-8c, AJL266-9c, and AJL330-6d as determined from these and other experiments. Size markers are shown at the right in each panel.

than those found in wild-type strains (Fig. 5) (31). Furthermore, a series of restriction enzymes recognizing 4-bp (*Bfa*I, *Nla*III, and *Rsa*I) or 6-bp (*Hin*dIII, *Xho*I, *Eco*RI, *Pst*I, and *Sca*I) sequences were unable to digest DNA distal to the telomeric *URA3* gene in either wild-type or *rap1*^{t} cells, consistent with the absence of nontelomeric DNA in these sequences (data not shown). It is unlikely that defects in position-independent processes (e.g., polymerase slippage) are responsible for this increase in tract size, since the size of an internal 80-bp poly($G_{1-3}T$) tract, introduced adjacent to the *URA3* gene, is identical in wild-type and *rap1-17* strains (Fig. 5).

Telomere instability and rapid deletion events in *rap1*^{t} cells. Two sets of observations indicate that the telomeres present in the *rap1*^{t} mutant cells are highly unstable. First, the distribution of tract sizes present at individual telomeres (i.e., the $cIII_L$ and cXI telomeres, as well as the *URA3*-marked telomere of chromosome V) is extremely heterogeneous. Unlike individual wild-type telomeres, which do not normally vary in size by more than 200 bp, telomeres in the population of *rap1*^{t} cells differ by up to 2 kb in size (Fig. 3, 5, and 6). Since each round of subculturing proceeds from a single cell containing a unique copy of each chromosome, the increased heterogeneity must be generated in less than 20 generations.

Second, unlike the telomeres of wild-type and *rap1-5* strains, the telomeres of *rap1*^{t} cells are susceptible to rapid deletions of telomeric tract sequences (Fig. 3 and 6). Following growth of *rap1*^{t} cells into colonies, we often observe two discrete telomeric distributions: one at the original size of the elongated telomeres in the parent strain, and a second centered at a smaller fragment size (e.g., spore colony 9c in Fig. 3). These events occur at high frequencies: 22% of *rap1-18* colonies (11 of 50) and 9% of *rap1-17* colonies (9 of 100) contain one or more deleted termini in addition to tracts of the original size (Fig. 6). Species up to 3 kb smaller than the original tract size (3 to 4 kb in these strains) are observed. When cells inheriting only the chromosome containing the truncated telomeres are subcultured, the telomeres slowly regain their elongated size (Fig. 3 and data not shown). These data suggest that a reversible deletion of a discrete number of telomeric repeats occurs in a subpopulation of *rap1*^{t} cells. Consistent with this hypothesis, colonies containing only the deleted form are also observed at similar frequencies (8 of 50 for *rap1-18* and 4 of 100 for *rap1-17*), as expected if deletion occurred in a subpopulation of cells prior to plating. Interestingly, in several cases, equal abundances of parental and deleted derivatives were observed. Since there is no difference in the growth rates of strains containing elongated and truncated $cIII_L$ telomeres, these data are most consistent with a single-step process occurring either early in colony growth, giving rise to equal abun-

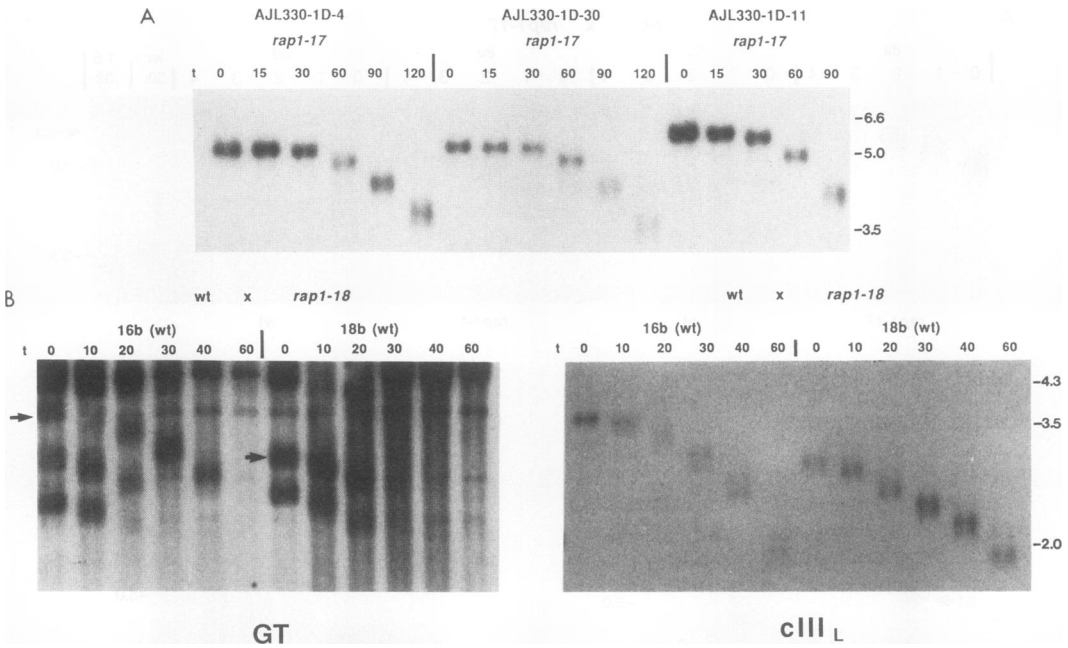

FIG. 4. Nuclease BAL 31 sensitivity of elongated telomeres. (A) DNA was isolated from subcultured progeny (colonies 4, 11, and 30) of a *rap1-17* spore colony (AJL330-1d) and digested with 0.2 U of nuclease BAL 31 per μg of DNA for 15 to 120 min, as indicated. The 0 lane refers to samples that did not receive the enzyme. The DNA was then digested with *Sal*I, and the blots were probed with the $cIII_L$ telomere-specific probe pKB1. Blots were stripped and reprobed with an *Nco*I-*Stu*I fragment of YCp120 (7), derived from a subtelomeric X repeat, that identifies both telomeric and subtelomeric fragments. As expected, multiple subtelomeric *Sal*I restriction fragments that were insensitive to digestion by nuclease BAL 31 were identified, demonstrating the specificity of this nuclease (data not shown). Size markers (in kilobases) are shown on the right. (B) DNA was isolated from the subcultured progeny of two wild-type (wt) spore colonies (AJL256-16b and AJL256-18b) derived from a diploid heterozygous for the *rap1-18* allele. DNA was digested with 0.6 U of nuclease BAL 31 per μg of DNA for 10 to 60 min, as indicated, and subsequently digested with *Sal*I. Lane 0 refers to samples that did not contain nuclease BAL 31. Blots were probed with pKB1 ($cIII_L$), stripped, and reprobed with poly(GT) (GT). The arrow on the left indicates the position of the $cIII_L$ telomere on the blot hybridized to poly(GT). In contrast to the telomeric species, internal poly(GT) tracts displayed on this blot were not sensitive to digestion by nuclease BAL 31. Note that although the telomere sizes of the $cIII_L$ telomeres inherited by the two wild-type spore colonies differ by 600 bp, the size at which hybridization is lost to poly(GT) is identical for both fragments. Similar results were obtained for spore colony AJL266-8c shown in Fig. 3 (data not shown).

dances of the two species, or later in colony growth, giving rise to substoichiometric species of smaller size. The deletions do not occur uniformly at all telomeres, since the majority of telomeres in these cells remain elongated (e.g., compare spore colony 9c in Fig. 2 and 3).

One possible pathway that may generate deleted termini is intrachromatid crossing over and gene conversion between telomere sequences, a process expected to be dependent on the *RAD1* and *RAD52* gene products (27, 56). However, the frequent appearance of deleted telomeres in *rad52 rad1 rap1-17* triple mutant cells (≈20% [9 of 49]; Fig. 3) makes this possibility unlikely.

Several observations suggest that the generation of rapid deletion events (RDEs) is a stochastic process. First, RDEs are not strongly dependent on telomeric tract size. These events can take place at any point during telomere elongation. Second, the amount of telomeric tract deleted varies from several hundred base pairs (the lowest significant shift in mobility in mutant cells) to >3 kb (Fig. 6A and C). Third, RDEs are not $cIII_L$ specific. A similar frequency of RDEs was observed at a second telomere, located on chromosome XI (Fig. 6B and D). Finally, RDEs appear to occur randomly at different chromosomal ends. Cells containing a deletion on chromosome XI only infrequently display a deletion at $cIII_L$ (3 of 18 events scored).

Both nondisjunction and chromosome loss events are enhanced in *rap1*^{t} cells. The instability of telomeres in the *rap1*^{t} mutant cells prompted us to determine whether chromosome stability is also influenced in these strains. To test this, we introduced a nonessential linear chromosome into wild-type, *rap1-5*, *rap1-17*, and *rap1-18* strains (53). This 150-kb artificial chromosome consists of an intact $cIII_L$ and a telocentric right arm that contains both the *URA3* and *SUP11* genes. The *SUP11* gene permits a visual assay for chromosome loss through suppression of the *ade2-1* ochre allele. Colonies lacking this chromosome appear red as a result of the accumulation of a red pigment in *ade2-1* cells, while wild-type strains containing the chromosome appear white. The results of chromosome loss assays in wild-type, *rap1-5*, and *rap1-17* haploid strains demonstrated that while wild-type and *rap1-5* cells have comparable loss rates, *rap1-17* cells have an ≈20-fold higher rate of chromosome loss (Table 1). Similar results were obtained for cells containing the *rap1-18* allele (data not shown). High chromosome loss rates are also observed in homozygous *rap1-17*/*rap1-17* diploids. Chromosome instability is recessive. When a CEN plasmid containing a wild-type copy of RAP1 is introduced into homozygous *rap1-17*/*rap1-17* diploids, significantly lower loss rates are observed (Table 1). Similarly, wild-type loss rates are observed in diploid strains heterozygous for *rap1-17* (data not shown).

We note that chromosome loss rates determined early and

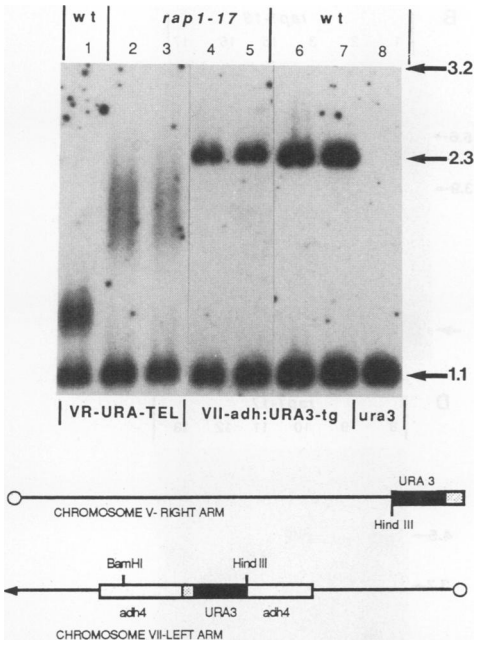

FIG. 5. Elongation of telomeric but not internal poly($G_{1-3}T$) tracts in *rap1-17* cells. In lanes 1 to 3, DNA was isolated from wild-type (wt) and *rap1-17* strains containing a truncated right arm of chromosome V terminated with *URA3* and poly($G_{1-3}T$) sequences (VR-URA-TEL) (13). DNA was then digested with *Hin*dIII, and the resulting blots were probed with *URA3* sequences. The 1.1-kb fragment represents the *ura3-1* gene located at its normal chromosomal position. The larger heterodisperse fragments are telomeric fragments containing the 1.1-kb *URA3* gene and distal poly($G_{1-3}T$) tracts. Lane 1 shows a wild-type strain containing the marked chromosome V telomere; lanes 2 and 3 show independent *rap1-17* strains containing the chromosome V truncation. In lanes 4 to 8, DNA was isolated from wild-type (wt) and *rap1-17* strains containing the *URA3* gene adjacent to 80 bp of poly($G_{1-3}T$) at an internal position on the left arm of chromosome VII (VII-adh:URA3-tg) (13). DNA was digested with *Hin*dIII and *Bam*HI, and the resulting blots were probed with *URA3* sequences. The 2.3-kb species represents the predicted internal fragment spanning the poly($G_{1-3}T$) tract. Strains used: lanes 4 and 5, *rap1-17* strains containing the internal poly($G_{1-3}T$) tract; lanes 6 and 7, wild-type strains containing the internal poly($G_{1-3}T$) tract; lane 8, an unmarked wild-type strain containing the *ura3-1* mutation. For both sets of experiments, DNA was isolated from cells without extensive subculturing. A partial restriction map of the marked chromosomes V and VII derivatives, derived from Gottschling et al. (13), is shown at the bottom. Poly($G_{1-3}T$) tracts are indicated by the stippled boxes.

late in subculturing are indistinguishable, even though the size of the $cIII_L$ telomere of the artificial chromosome increases substantially during subculturing (data not shown). Hence, telomere tract elongation per se is probably not responsible for the elevated chromosome loss rates in these strains.

Two classes of aberrant chromosome segregation may contribute to these enhanced loss rates: 1:0 segregation, representing either a failure in replication or the physical loss of the chromosome from the nucleus, and 2:0 segregation patterns, most likely representing chromosome nondisjunction. In *rap1^t* haploid cells, *SUP11* ochre suppression is reduced. Two copies of *SUP11* are required for full suppression, giving rise to white colonies, while one copy of *SUP11* produces a pink colony (see Materials and Methods). This fortuitous ability to distinguish the copy number of the artificial chromosome in *rap1^t* cells permits the analysis of half sectors in the haploid state. Both 1:0 (pink:red) and 2:0 (white:red) segregation defects contribute to the overall increase in chromosome loss rates of *rap1-17* mutants. Similar sectoring frequencies were found in diploid *rap1-17*/*rap1-17* cells (Table 1). In contrast, sectoring frequencies of wild-type diploid cells are significantly lower, with most (16 of 17) of the interpretable sectors representing 2:0 segregation events, as expected from previous studies (38).

The *rap1^t* alleles produce C-terminal truncations of the RAP1 protein. To determine the mutations within the *RAP1* gene responsible for these phenotypes, we cloned and sequenced each of the *rap1^t* genes. To first test whether the cloned genes are able to confer the *rap1^t* phenotypes, we transformed CEN plasmids containing each *rap1^t* gene into a strain carrying both a deletion of the *RAP1* gene at its chromosomal position and a second CEN plasmid containing a wild-type *RAP1* gene. Following a plasmid shuffle, strains that contained only the cloned *rap1^t* genes were identified and characterized. The telomere lengths of each of the cloned *rap1^t* alleles were indistinguishable from those observed in the original *rap1^t* alleles at both 25 and 37°C (Fig. 7). These strains also displayed the slow growth rate and the down regulation of *SUP11* ochre suppression observed in the original strains (data not shown). Chromosome loss rates were also elevated, although to a lesser extent than in the original *rap1^t* strains, a likely consequence of a reduced penetrance of the plasmid-encoded products (data not shown).

Further subcloning defined a 1.2-kb region encompassing the C terminus of RAP1 that contains each of the *rap1^t* mutations. In each case, when the mutant *Sph*I-*Xba*I fragment was used to replace the same fragment of a *rap1-5* gene, the *rap1^t* phenotypes were recovered (Fig. 7B). Sequencing of the cloned genes demonstrated that each allele is the consequence of a nonsense mutation within a discrete region of the *RAP1* gene (Fig. 8). Sequencing of the *Sph*I-*Xba*I fragment from the *rap1-17* gene indicated the presence of only two mutations: a missense mutation (changing a proline to a leucine) at amino acid 661, followed immediately by a second frameshift mutation creating a UGA (opal) stop codon at amino acid 663. This mutation is therefore expected to give rise to a truncated protein of 662 amino acids, significantly smaller than the 827-amino-acid wild-type product. In the case of *rap1-19*, a point mutation is present that changes amino acid 665 from TAT to a TAA ochre stop codon, predicting a protein of 664 amino acids. The third allele, *rap1-18*, represents a change of TAT to TAG at amino acid 684, producing an amber nonsense codon and predicting a protein of 683 amino acids. This allele also has a second change at amino acid 673 (R to A) that appears to be a polymorphism present in several cloned *RAP1* genes (data not shown). No other mutations were present between the *Sph*I site and the nonsense mutations. Each nonsense mutation maps downstream of the DNA binding domain between amino acids 360 and 594 (23) and upstream of the original *rap1-5* mutation at amino acid 694, predicting a mutant protein capable of DNA binding but lacking the *rap1-5* lesion.

To test directly for the presence of truncated RAP1 derivatives in the *rap1^t* extracts, we performed Western analysis of wild-type and mutant extracts, using antibodies directed against wild-type RAP1 (Fig. 9A). The 97-kDa wild-type protein migrates anomalously at 120 kDa on SDS-polyacrylamide gels, as expected (50). Several low-abundance degradation products of RAP1, previously described (50), are also present in this extract. The RAP1 protein

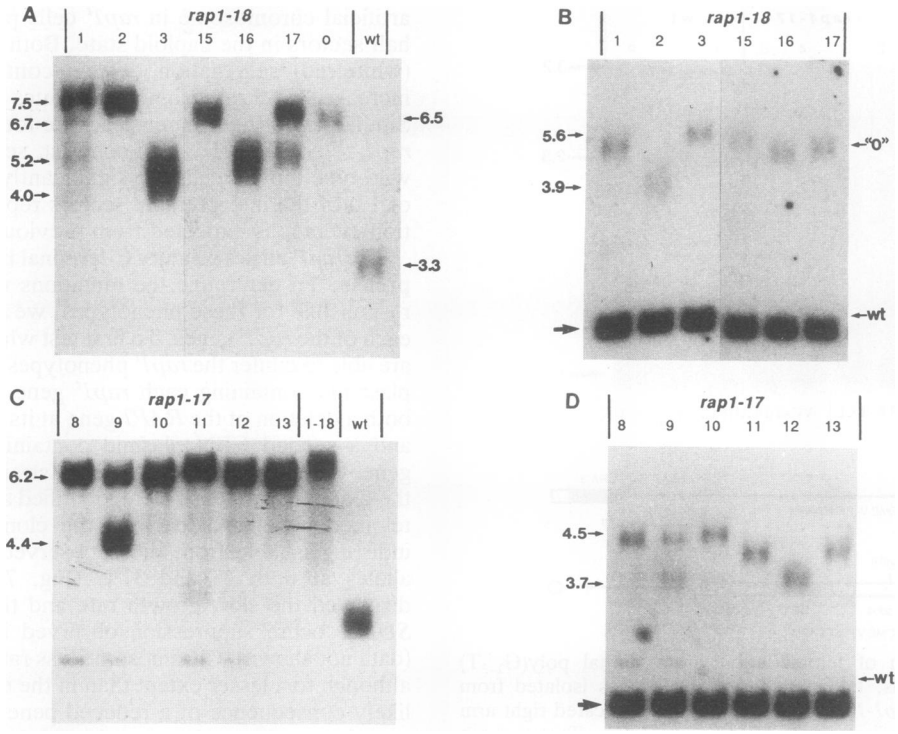

FIG. 6. RDEs in *rap1*^{t} cells. A *rap1-18* (A and B) or *rap1-17* (C and D) spore colony (AJL256-16d or AJL330-1d, respectively) derived from diploids heterozygous for each allele was subcultured for ≈100 generations, and the subcultured cells were plated on rich medium. DNA was isolated from 50 individual colonies from each strain (as well as an additional 50 colonies from a second *rap1-17* strain not shown), and the DNA was digested with *Sal*I. Blots were subsequently probed with pKB1 (cIII$_L$; A and C), stripped, and reprobed with pKB2 (cXI; B and D). pKB2 hybridizes predominantly to an internal fragment on cIII$_L$ (shown by the bold arrow) but, in addition, hybridizes more weakly to a telomeric fragment from chromosome XI. The results obtained from several representative colonies (1 to 3 and 15 to 17 for *rap1-18*; 8 to 13 for *rap1-17*) are shown. Also shown in panel A is DNA isolated from wild-type strains (lane wt) and the *rap1-18* strain before plating (lane 0). Arrows indicate the estimated sizes (in kilobases) of the different telomeric fragments as determined from these and other experiments. Arrows on the right in panels B and D indicate the positions both of the wild-type (wt) and of *rap1-18* ("0") cXI telomeric fragments before plating.

produced by two of the mutant strains, *rap1-17* and *rap1-19*, both predicted to be 74 kDa, migrate at identical mobilities at 94 kDa, consistent with a loss of 163 to 165 amino acids. In contrast, *rap1-18*, which is expected to produce a slightly longer protein of 76 kDa, gives rise to a species of 96 kDa, consistent with the loss of 144 amino acids.

Another indication of the presence of truncated proteins in the *rap1*^{t} alleles comes from the comparison of RAP1-DNA complexes in extracts isolated from both wild-type and *rap1*^{t} cells (Fig. 9B). While comparable levels of binding to telomeric oligonucleotides containing RAP1 binding sites were observed in both mutant and wild-type extracts, RAP1^t-DNA complexes migrate more rapidly than do wild-type complexes, consistent with the production of a truncated RAP1^t protein in vivo. Binding of the RAP1^t proteins is specific: competition of binding is achieved only with oligonucleotides containing intact telomeric (AT13) or nontelomeric (TEF2) RAP1 binding sites (data not shown).

DISCUSSION

Degregulation of multiple telomeric processes in *rap1*^{t} alleles. In this study, we have characterized three novel alleles of *RAP1*. Each allele produces a truncated RAP1 molecule

TABLE 1. Elevated chromosome loss rates in *rap1-17* cells

Genotype (no. of trials)	Fluctuation rate[a] (10^{-4} events/cell division)	Half-sector rates[b] (10^{-4} events/cell division)		
		2:0	1:0	Total
RAP1 (5)	0.70 (±0.43)	NA	NA	1.00 (101)
rap1-5 (2)	0.94 (±0.13)	NA	NA	1.08 (77)
rap1-17 (9)	20.60 (±10.40)	8.9 (134)	2.2 (33)	11.10 (167)
RAP1/RAP1 (3)	1.61 (±1.28)	ND	ND	1.13 (51)
rap1-17/rap1-17	2.30 (±1.20)	ND	ND	ND
CEN(*RAP1*) (2)				
rap1-17/rap1-17 (5)	29.00 (±10.60)	11.8 (165)	4.2 (59)	16.00 (224)

[a] Ranges of values observed in independent trials are given in parentheses. Standard deviations at 95% confidence, calculated for samples subjected to more than three trials, were 0.37×10^{-4}, 5.3×10^{-4}, and 7.70×10^{-4} for *RAP1*, *rap1-17*, and *rap1-17/rap1-17* cells, respectively.

[b] Numbers of sectors analyzed are given in parentheses. ND, not determined; NA, not applicable.

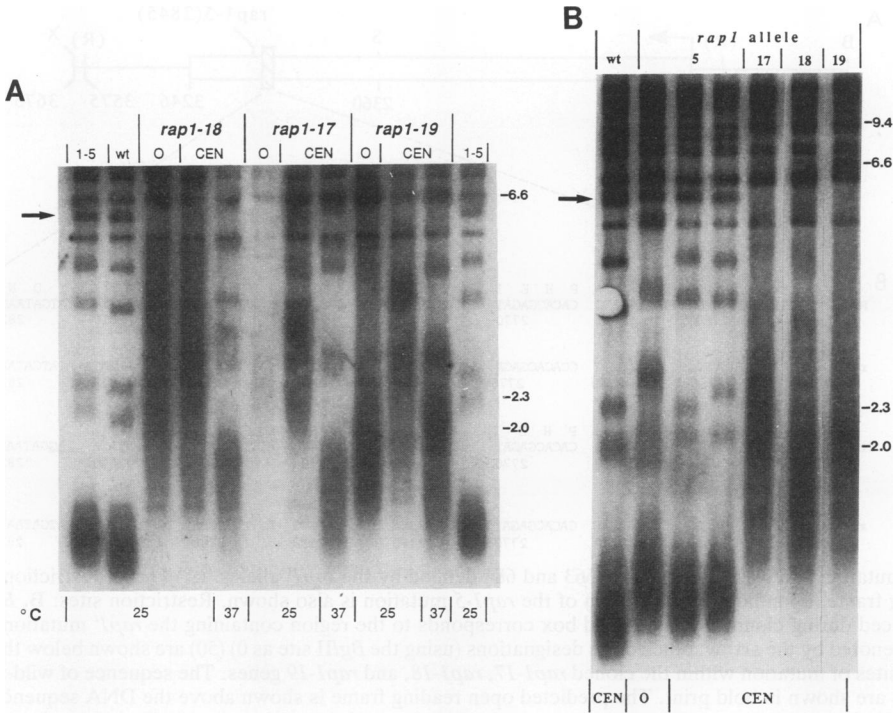

FIG. 7. Phenotypes of cloned *rap1*^{t} alleles. (A) The cloned *rap1*^{t} alleles confer temperature-sensitive telomere elongation. Strains (GK15, GK16, and GK17) containing each of the cloned *rap1*^{t} genes as the sole source of RAP1 on a CEN plasmid (CEN) were subcultured for 100 generations at either 25 or 37°C. DNA was isolated from each of these strains after the last round of subculturing as well as from the original *rap1-17*, *rap1-18*, and *rap1-19* (o) strains subcultured at 25°C. DNA was digested with *Xho*I, and blots were probed with poly(GT). The results obtained with wild-type (wt) and *rap1-5* (1-5) strains grown at 25°C are also shown. The arrow on the left indicates the position of the $cIII_L$ *Xho*I-terminal restriction fragment, which also elongates in strains containing the cloned *rap1*^{t} alleles. Temperatures of growth for each strain are shown at the bottom. Size markers (in kilobases) are indicated on the right. (B) The *rap1*^{t} alleles map to the terminal 1.2 kb of the RAP1 gene. The *Sph*I-*Xba*I fragment of each *rap1*^{t} allele (*rap1-17*, *rap1-18*, and *rap1-19*) was used to replace the corresponding fragment of a *rap1-5* allele, and the resulting hybrid genes were introduced into strains on CEN plasmids (CEN) as the sole source of RAP1. DNA was isolated from these strains (GK19, GK20, and GK21) as well as from strains containing a cloned wild-type (wt; GK18) or *rap1-5* (GK22) gene on a CEN plasmid. DNA was digested with *Xho*I, and blots were probed with poly(GT). Also shown are the results obtained with an original (o) *rap1-5*-containing strain. The arrow on the left corresponds to the position of the $cIII_L$ *Xho*I telomeric restriction fragment. Size markers (in kilobases) are indicated on the right.

that, while capable of efficient and specific binding to DNA, lacks the C-terminal 144 to 165 amino acids. The *rap1*^{t} alleles result in promiscuous telomere elongation and instability, slow growth, and high rates of chromosome loss. Interestingly, while these alleles are recessive for both the increased frequency of chromosome loss and slow growth, their telomeric length effects are semidominant in heterozygous diploids. Thus, unlike the previously described recessive alleles of *rap1* (35), these alleles are likely to act by antagonizing or interfering with the telomere elongation machinery. The phenotypes observed in the *rap1*^{t} alleles suggest the simultaneous deregulation of multiple processes acting at the telomere in *rap1*^{t} strains.

(i) Telomere elongation. Telomere tracts in *rap1*^{t} cells grown at 25°C increase in size up to 4 kb larger than telomeres found in wild-type or *rap1-5* cells. Such telomere elongation is the likely consequence of an increase in the activity or processiveness of telomere addition enzymes (e.g., telomerase) on *rap1*^{t} telomeric substrates. The alternative possibility, that telomeres are more resistant to mechanisms of telomere loss, seems unlikely given the instability of telomeres in these strains. We note that although the *rap1-5* mutation is not present in the RAP1^t protein, telomere elongation is nonetheless temperature sensitive. This finding indicates that a function important for telomere elongation is impaired at 37°C, an effect which may be mediated through partial unfolding of the protein at higher temperatures.

The characteristics of telomere fragment elongation in *rap1*^{t} strains indicate that most increases in telomere size are the consequence of elongation of poly($G_{1-3}T$) sequences. Nonetheless, we have also observed the presence of apparently irreversible changes in telomeric fragment sizes. These events have been identified when *rap1*^{t} telomeres are stabilized at an increased size in a wild-type background or in heterozygous diploids (e.g., spore colonies 8b in Fig. 3 and 16b in Fig. 4). When testable, this increase in fragment length appears to be the consequence of an increase in telomere tract size, as defined by nuclease BAL 31 digestion (Fig. 4). This effect is unlikely to be the consequence of a second linked mutation, since many telomeres of these cells decrease to sizes close to or at wild-type tract lengths. In addition, this phenotype has been observed in two independently derived alleles, *rap1-17* and *rap1-18*. Whether this effect is the consequence of a rearranged or scrambled telomeric tract or of a stably maintained change in chromatin structure is currently under investigation.

(ii) Telomere tract heterogeneity and RDEs. In wild-type cells the equilibrium between telomere elongation and loss is regulated, with the length of an individual telomere varying

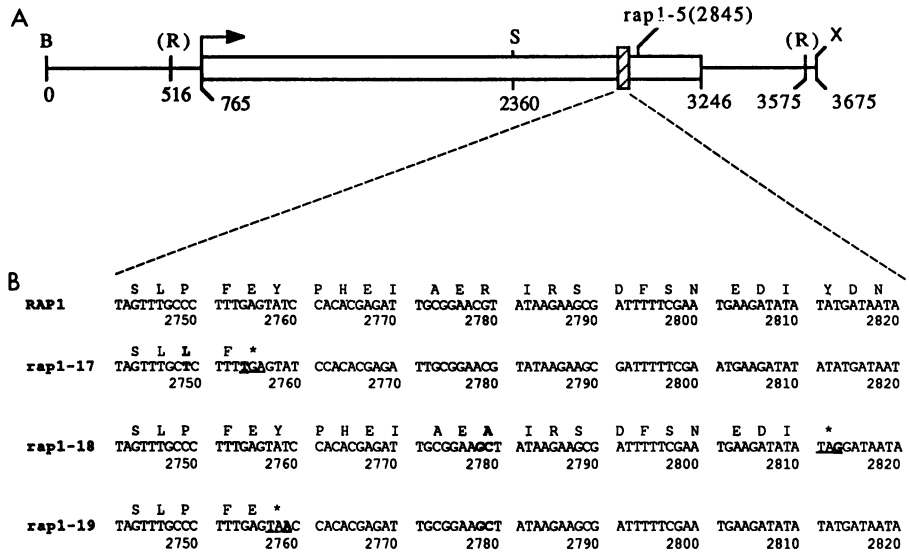

FIG. 8. Nonsense mutations between amino acids 663 and 684 defined by the *rap1*^{t} alleles. (A) Partial restriction map of *RAP1* showing the *RAP1* open reading frame (open box). The position of the *rap1-5* mutation is also shown. Restriction sites: B, *Bgl*II; S, *Sph*I; X, *Xba*I; (R), *Eco*RI site introduced during cloning. The hatched box corresponds to the region containing the *rap1*^{t} mutations. The beginning of the open reading frame is denoted by the arrow. Nucleotide designations (using the *Bgl*II site as 0) (50) are shown below the map. (B) Partial DNA sequence showing the sites of mutation within the cloned *rap1-17*, *rap1-18*, and *rap1-19* genes. The sequence of wild-type *RAP1* is shown for comparison. Mutations are shown in bold print. The predicted open reading frame is shown above the DNA sequence; mutated amino acids are in bold print. No other mutations were present between the *Sph*I site and the stop codon (indicated by the asterisks and underlined sequences) in any of the alleles.

by no more than 100 bp from the average tract length. In contrast, telomeres in *rap1*^{t} cells are highly unstable. This instability is manifested both by the rapid generation of telomere tract heterogeneity and by the susceptibility of telomeres to terminal deletion, a process not previously observed in yeast cells. Interestingly, telomeric deletion in *rap1*^{t} cells appears to act randomly with regard to the chromosome affected, the length of the substrate, and the extent of the deletion. In this regard, we note that rapid deletion events may, at a low frequency, delete the telomere tract beyond a critical size necessary for subsequent telomere addition or function, possibly resulting in the high rate of chromosome nondisjunction and loss observed in these mutants.

Telomere instability could be the consequence of an inherent instability of long telomeres or, alternatively, a more direct result of altered RAP1 function at the telomere. Consistent with the former possibility is the observation that another mutation causing elongated telomere tracts, *cdc17*, also produces a moderate increase in heterogeneity (6; data not shown). However, the observations that wild-type cells inheriting elongated cIII$_L$ telomeres exhibit neither the heterogeneity (e.g., compare spore colonies 8b and 8c in Fig. 3) nor the RDEs (data not shown) generated by *rap1*^{t} telomeres, despite their apparently identical tract sizes, are inconsistent with a size-dependent model. Further studies will be necessary to distinguish between these possibilities.

A number of mechanisms can explain the presence of RDEs. First, poly(G_{1-3}T) tracts in the *rap1*^{t} strains may be more susceptible to endonucleolytic cleavage, possibly as a result of an increase in the number of nicks, gaps, or double-strand breaks present at the telomere (55). Alkaline gels of the elongated cIII$_L$ telomeres have revealed a distribution of fragment sizes very similar to that of telomeres fractionated on native agarose gels (29). Thus, any increase in such DNA damage must be restricted to sites close to the terminus or to a subpopulation of telomeres. We note that the data are also consistent with a rapid exonucleolytic loss of a discrete number of repeats occurring in a subpopulation of telomeres.

Second, several classes of recombination events between telomeric tracts could give rise to RDEs. One potential mechanism, unequal sister chromatid exchange, would be expected to give rise to two chromatids of different sizes and is inconsistent with our failure to detect the expected reciprocal product. An alternative mechanism, intrachromatid crossing over or gene conversion, is not supported by the observation that *rad1 rad52 rap1-17* triple mutants do not exhibit a reduced frequency of RDEs (27, 56). A third, more attractive pathway is the *rad52*-independent cut-and-paste mechanism that has been proposed to explain intrachromatid recombination between rDNA repeats (40). In this model, recombination is initiated by strand breakage, followed by strand recision and misalignment, ultimately giving rise to a simple excision event without the generation of the reciprocal product.

We have previously noted that the ability of mutants defective in telomere addition to attain stable equilibria centered at reduced tract sizes predicts a cellular mechanism of telomere loss that may be sensitive to tract length (36). In contrast to RNA primer loss and exonucleolytic degradation, such a mechanism of loss, possibly involving endonucleolytic cleavage or intrachromatid recombination, would increase in probability as telomeres elongated, thereby providing a simple stochastic means of telomere size control. Given the correlation between the presence of RDEs and increased tract heterogeneity in *rap1*^{t} cells, we suggest that RDEs may serve as such a stochastic sizing mechanism in wild-type cells.

Taken together, the phenotypes of both recessive and

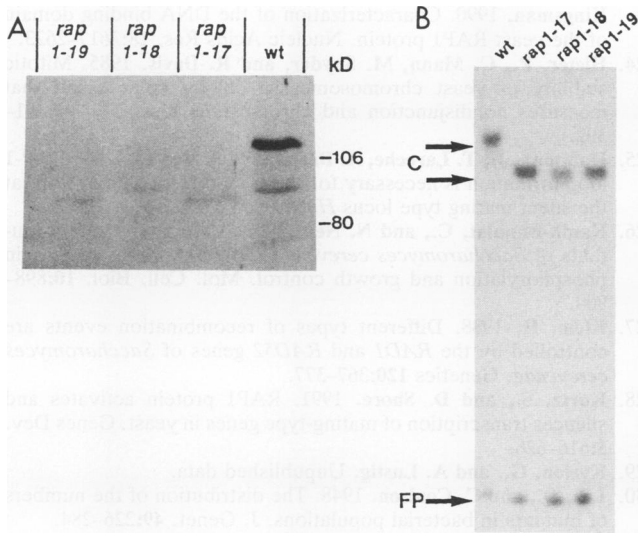

FIG. 9. Truncated versions of RAP1 produced by the *rap1^t* alleles. (A) Western analysis of extracts isolated from strains containing either cloned wild-type (wt) (GK18), *rap1-17* (GK19), *rap1-18* (GK20), or *rap1-19* (GK21) gene as the sole source of RAP1, using antibodies directed against RAP1. The additional species in the wild-type lane are degradation products of RAP1. Molecular weight standards are shown on the right. (B) Truncated *RAP1^t* proteins form complexes with DNA in vitro. Extracts isolated from wild-type (wt), *rap1-17*, *rap1-18*, and *rap1-19* strains were incubated with ^{32}P-labeled AT13, and the products were fractionated by native polyacrylamide gel electrophoresis. The positions of the free probe (FP) and DNA-protein complexes (C) are indicated on the left. In each case, the RAP1^t-DNA complexes migrate more rapidly than do wild-type complexes. Identical results were obtained with extracts isolated from both the original *rap1^t*-containing strains and strains carrying the cloned *rap1^t* alleles as the sole source of RAP1. Identical results were also obtained with AT1 (35), a telomeric oligonucleotide that contains two perfect matches to the RAP1 consensus sequence, and TEF2 (4), an oligonucleotide that contains a nontelomeric RAP1 binding site (data not shown).

semidominant alleles of *RAP1*, as well as physical evidence that RAP1 binds to the telomere in vivo (58), suggest that RAP1 is an intrinsic functional component of the telomere. Given the multiple effects of the *rap1^t* alleles on telomere addition and stability, it is also difficult to explain these effects as the failure to activate a set of genes important for telomere regulation. However, these possibilities will be distinguished only through the identification of factors that are necessary for the telomeric functions of RAP1.

The domain structure of RAP1. Two previous studies have suggested that the C terminus of RAP1 may be important for telomere length control. First, mutations within the C terminus of RAP1 that affect silencing (the *rap1^s* alleles) also cause a 100- to 300-bp elongation in telomere tract size (54). Second, overproduction of the C terminus of RAP1 also results in the generation of similarly elongated telomeres (8). Interestingly, overproduction of full-length RAP1, but not the C terminus of RAP1, also confers a loss of mitotic chromosome stability (8), suggesting that the factors titrated by the C terminus are different from those required for maintaining chromosome stability.

The C-terminal truncations of RAP1 described in this study clearly demonstrate that the C terminus is dispensable for viability. Although growth rates are twofold lower than in the wild type, this difference appears to be the consequence of an increase in cell cycle length rather than a high level of cell death (data not shown). However, while not affecting either viability or DNA binding, deletion of the terminal 144 to 165 amino acids confers extensive phenotypes on telomere length and stability, chromosome stability, and telomeric gene expression (31). These studies therefore suggest that the role of the C-terminal domain in these processes is more extensive than indicated by previous overproduction and mutational analyses (8, 35, 58).

One surprising finding is that the RAP1^t protein is truncated within the putative activation domain (between amino acids 630 and 695) (20), raising the possibility either that the domain as mapped by hybrid GAL4-RAP1 protein fusions does not fully reflect the domain within its normal context or that the residual activation of the truncated domain is sufficient for viability. Of course, a third possibility, that transcriptional activation is not the essential function of RAP1, should also be considered.

Models for RAP1 action at telomeres. Several models of RAP1 action are consistent with the phenotypes observed in the *rap1^t* alleles. First, the RAP1^t protein may be unable to associate with proteins required for limiting the activities of replication, recombination, and degradation enzymes. If the C terminus of *RAP1* is required for these associations, then the inability of RAP1^t to bind to these factors may result in promiscuous telomere elongation and deletion. One of these factors may be the C-terminus-binding factor RIF1, which itself influences telomere elongation and silencing to a similar extent as do the *rap1^s* alleles (21). However, the absence of RIF1 interaction cannot alone explain the phenotypes of the *rap1^t* alleles, since the susceptibility of *rap1^t* telomeres to elongation and deletion is substantially greater than that found in *rif1* mutant cells.

A second possibility is that the truncated RAP1 molecules cannot assemble properly into telomeric chromatin. The telomeric DNA may then be more susceptible to telomere elongation and degradation activities. Such a defect could be mediated either directly through an altered structure of RAP1^t-DNA complexes or through the inability of other factors to bind to the yeast telomere in the absence of the C terminus of RAP1. Consistent with this possibility is the finding that another process, the position-dependent repression of telomeric gene expression observed in wild-type cells (13), is relieved in *rap1^t* cells (31).

Alternatively, the C terminus of RAP1 may serve as a region required for association with a specific nuclear substructure, such as the nuclear scaffold. RAP1 has been identified biochemically to be a component of the nuclear scaffold, and it is capable of looping DNA in vitro, a characteristic of scaffold proteins (25). Interestingly, telomeric sequences, at least in human cells, are also associated with the scaffold (10). Conceivably, failure of RAP1^t binding to the nuclear scaffold could restrict the accessibility of factors normally involved in maintaining telomere stability. Further studies on the factors that interact with the C terminus in vivo and the chromatin structure of telomeres in *rap1^t* cells should begin to unravel the basis of RAP1 action in regulating telomere size, stability, and function.

ACKNOWLEDGMENTS

We thank D. Gottschling, P. Hieter, C. Newlon, R. Rothstein, D. Shore, B.-K. Tye, and V. Zakian for providing plasmids and D. Gottschling for communicating results prior to publication. We also thank T. deLange and E. B. Hoffman for critical reading of the manuscript.

These studies were supported by grants from the American Cancer Society (MV 446) and the National Science Foundation (DMB 9120208).

REFERENCES

1. **Ausubel, F., R. Brent, R. Kingston, D. Moore, J. Smith, J. Seidman, and K. Struhl. (ed.).** 1987. Current protocols in molecular biology. John Wiley & Sons, New York.
2. **Blackburn, E., and S. Chiou.** 1981. Non-nucleosomal packaging of a tandemly repeated DNA sequence at termini of extrachromosomal DNA coding for rRNA in *Tetrahymena*. Proc. Natl. Acad. Sci. USA **78**:2263–2267.
3. **Boeke, J., J. Trueheart, G. Natsoulis, and G. Fink.** 1987. 5-Fluoro-orotic acid as a selective agent in yeast molecular genetics. Methods Enzymol. **154**:164–175.
4. **Buchman, A., N. Lue., and R. Kornberg.** 1988. Connections between transcriptional activators, silencers, and telomeres as revealed by functional analysis of a yeast DNA-binding protein. Mol. Cell. Biol. **8**:5086–5099.
5. **Budarf, M., and E. Blackburn.** 1986. Chromatin structure of the telomeric region and 3′-nontranscribed spacer of *Tetrahymena* ribosomal RNA genes. J. Biol. Chem. **261**:363–369.
6. **Carson, M., and L. Hartwell.** 1985. CDC17: an essential gene that prevents telomere elongation in yeast. Cell **42**:249–257.
7. **Chan, C., and B.-K. Tye.** 1983. Organization of DNA sequences and replication origins at yeast telomeres. Cell **33**:563–573.
8. **Conrad, M., J. Wright, A. Wolf, and V. Zakian.** 1990. RAP1 protein interacts with yeast telomeres in vivo: overproduction alters telomere structure and decreases chromosome stability. Cell **63**:739–750.
9. **Coren, J., E. Epstein, and V. Vogt.** 1991. Characterization of a telomere-binding protein from *Physarum polycephalum*. Mol. Cell. Biol. **11**:2282–2290.
10. **deLange, T.** 1992. Human telomeres are attached to the nuclear matrix. EMBO J. **11**:717–724.
11. **Gardiner, K., and D. Patterson.** 1988. Transverse alternating field electrophoresis. Nature (London) **331**:371–372.
12. **Giesman, D., L. Best, and K. Tatchell.** 1991. Role of RAP1 in the regulation of *MATα* locus. Mol. Cell. Biol. **11**:1069–1079.
13. **Gottschling, D., O. Aparicio, B. Billington, and V. Zakian.** 1990. Position effect at *S. cerevisiae* telomeres: reversible repression of Pol II transcription. Cell **63**:751–762.
14. **Gottschling, D., and V. Zakian.** 1986. Telomere proteins: specific recognition and protection of the natural termini of *Oxytricha* macronuclear DNA. Cell **47**:195–205.
15. **Gottschling, D., and T. Cech.** 1984. Chromatin structure of the molecular ends of *Oxytricha* macronuclear DNA: phased nucleosomes and a telomeric complex. Cell **38**:501–510.
16. **Greider, C., and E. Blackburn.** 1985. Identification of a specific telomere terminal transferase activity in *Tetrahymena* extracts. Cell **43**:405–413.
17. **Greider, C., and E. Blackburn.** 1987. The telomere terminal transferase of *Tetrahymena* is a ribonucleoprotein enzyme with two kinds of primer specificity. Cell **51**:887–898.
18. **Greider, C., and E. Blackburn.** 1989. A telomeric sequence in the RNA of *Tetrahymena* telomerase required for telomere repeat synthesis. Nature (London) **337**:331–337.
19. **Gualberto, A., R. Patrick, and K. Walsh.** 1992. Nucleic acid specificity of a vertebrate telomere-binding protein: evidence for G-G base pair recognition at the core-binding site. Genes Dev. **6**:815–824.
20. **Hardy, C., D. Balderes, and D. Shore.** 1992. Dissection of a carboxy-terminal region of the yeast regulatory protein RAP1 with effects on both transcriptional activation and silencing. Mol. Cell. Biol. **12**:1209–1217.
21. **Hardy, C., L. Sussel, and D. Shore.** 1992. A RAP1-interaction protein involved in transcriptional silencing and telomere length regulation. Genes Dev. **6**:801–814.
22. **Hegemann, J., J. Shero, G. Cottarel, P. Philippsen, and P. Hieter.** 1988. Mutational analysis of centromere DNA from chromosome VI of *Saccharomyces cerevisiae*. Mol. Cell. Biol. **8**:2523–2535.
23. **Henry, Y., A. Chambers, J. Tsang, A. Kingsman, and S. Kingsman.** 1990. Characterization of the DNA binding domain of the yeast RAP1 protein. Nucleic Acids Res. **18**:2617–2623.
24. **Hieter, P., C. Mann, M. Snyder, and R. Davis.** 1985. Mitotic stability of yeast chromosomes: a colony color assay that measures nondisjunction and chromosome loss. Cell **40**:381–392.
25. **Hofmann, J., T. Laroche, A. Brand, and S. Gasser.** 1989. RAP-1 loop formation is necessary for DNA loop formation in vitro at the silent mating type locus *HML*. Cell **57**:725–737.
26. **Kanik-Ennulat, C., and N. Neff.** 1990. Vanadate-resistant mutants of *Saccharomyces cerevisiae* show alterations in protein phosphorylation and growth control. Mol. Cell. Biol. **10**:898–909.
27. **Klein, H.** 1988. Different types of recombination events are controlled by the *RAD1* and *RAD52* genes of *Saccharomyces cerevisiae*. Genetics **120**:367–377.
28. **Kurtz, S., and D. Shore.** 1991. RAP1 protein activates and silences transcription of mating-type genes in yeast. Genes Dev. **5**:616–628.
29. **Kyrion, G., and A. Lustig.** Unpublished data.
30. **Lea, D., and C. Coulson.** 1948. The distribution of the numbers of mutants in bacterial populations. J. Genet. **49**:226–284.
31. **Liu, K., and A. Lustig.** 1992. Unpublished data.
32. **Liu, Z., and B.-K. Tye.** 1991. A yeast protein that binds to vertebrate telomeres and conserved telomeric junctions in yeast. Genes Dev. **5**:49–59.
33. **Longtine, M., N. Wilson, M. Petracek, and J. Berman.** 1989. A yeast telomere binding activity binds to two related telomere sequence motifs and is indistinguishable from RAP1. Curr. Genet. **6**:225–240.
34. **Lundblad, V., and J. Szostak.** 1989. A mutant with a defect in telomere elongation leads to senescence in yeast. Cell **57**:633–643.
35. **Lustig, A., S. Kurtz, and D. Shore.** 1990. Involvement of the silencer and UAS binding protein RAP1 in regulation of telomere length. Science **250**:549–553.
36. **Lustig, A., and T. Petes.** 1986. Identification of yeast mutants with altered telomere structure. Proc. Natl. Acad. Sci. USA **83**:1398–1402.
37. **Morin, G.** 1989. The human telomere terminal transferase enzyme is a ribonucleoprotein that synthesizes TTAGGG repeats. Cell **59**:521–529.
38. **Murray, A., N. Schultes, and J. Szostak.** 1986. Chromosome length controls mitotic chromosome segregation in yeast. Cell **45**:529–536.
39. **Oliver, S., et al.** 1992. The complete DNA sequence of yeast chromosome III. Nature (London) **357**:38–46.
40. **Ozenberger, B., and G. S. Roeder.** 1991. A unique pathway of double-strand break repair operates in tandemly repeated genes. Mol. Cell. Biol. **11**:1222–1231.
41. **Price, C.** 1990. Telomere structure in *Euplotes crassus*: characterization of DNA-protein interactions and isolation of a telomere-binding protein. Mol. Cell. Biol. **10**:3421–3431.
42. **Price, C., and T. Cech.** 1987. Telomeric DNA-protein interactions of *Oxytricha* macronuclear DNA. Genes Dev. **1**:783–793.
43. **Raghuraman, M., and T. Cech.** 1989. Assembly and self-association of *Oxytricha* telomeric nucleoprotein complexes. Cell **59**:719–728.
44. **Raghuraman, M., C. Dunn, B. Hicke, and T. Cech.** 1989. *Oxytricha* telomeric nucleoprotein complexes reconstituted with synthetic DNA. Nucleic Acids Res. **17**:4235–4253.
45. **Shampay, J., and E. Blackburn.** 1988. Generation of telomere-length heterogeneity in *Saccharomyces cerevisiae*. Proc. Natl. Acad. Sci. USA **85**:534–538.
46. **Shampay, J., J. Szostak, and E. Blackburn.** 1984. DNA sequences of telomeres maintained in yeast. Nature (London) **310**:154–157.
47. **Sherman, F., G. Fink, and J. Hicks.** 1986. Methods in yeast genetics. Cold Spring Harbor Laboratory, Cold Spring Harbor, N.Y.
48. **Shippen-Lentz, D., and E. Blackburn.** 1989. Telomere terminal transferase activity from *Euplotes crassus* adds large numbers of TTTTGGGG repeats onto telomeric primers. Mol. Cell. Biol.

9:2761–2764.
49. **Shippen-Lentz, D., and E. Blackburn.** 1990. Functional evidence for an RNA template in telomerase. Science **247**:546–552.
50. **Shore, D., and K. Nasmyth.** 1987. Purification and cloning of a DNA binding protein from yeast that binds to both silencer and activator elements. Cell **51**:721–732.
51. **Shore, D., D. Stillman, A. Brand, and K. Nasmyth.** 1987. Identification of silencer binding proteins from yeast: possible roles in *SIR* control and DNA replication. EMBO J. **6**:461–467.
52. **Sikorski, R., and P. Hieter.** 1989. A system of shuttle vectors and yeast host strains designed for efficient manipulation of DNA in *Saccharomyces cerevisiae*. Genetics **122**:19–27.
53. **Spencer, F., C. Connelly, S. Lee, and P. Hieter.** 1988. Isolation and cloning of conditionally lethal chromosome transmission fidelity genes in *Saccharomyces cerevisiae*. Cancer Cells **6**:441–452.
54. **Sussel, L., and D. Shore.** 1991. Separation of transcriptional activation and silencing functions of the *RAP1*-encoded repressor/activator protein 1: isolation of viable mutants affecting both silencing and telomere length. Proc. Natl. Acad. Sci. USA **88**:7749–7753.
55. **Szostak, J., and E. Blackburn.** 1982. Cloning yeast telomeres on linear plasmid vectors. Cell **29**:245–255.
56. **Thomas, B., and R. Rothstein.** 1989. The genetic control of direct-repeat recombination in *Saccharomyces*: the effect of *rad52* and *rad1* on mitotic recombination at *GAL10*, a transcriptionally regulated gene. Genetics **123**:725–738.
57. **Walmsley, R., and T. Petes.** 1985. Genetic control of chromosome length in yeast. Proc. Natl. Acad. Sci. USA **82**:506–510.
58. **Wright, J., D. Gottschling, and V. Zakian.** 1992. *Saccharomyces* telomeres assume a non-nucleosomal chromatin structure. Genes Dev. **6**:197–210.
59. **Zahler, A., and D. Prescott.** 1988. Telomere terminal transferase activity in the hypotrichous ciliate *Oxytricha nova* and a model for replication of the ends of linear DNA molecules. Nucleic Acids Res. **16**:6953–6972.
60. **Zakian, V.** 1989. Structure and function of telomeres. Annu. Rev. Genet. **23**:579–604.